## Title
Endovascular Biopsy: Evaluating the Feasibility of Harvesting Endothelial Cells Using Detachable Coils



## Journal
Interventional Neuroradiology, 19(4)

## ISSN
1591-0199

## Authors
Cooke, Daniel L
Su, Hua
Sun, Zhengda
et al.

## Publication Date
2013-12-01

## DOI
10.1177/159101991301900401

Peer reviewed

# Endovascular Biopsy: Evaluating the Feasibility of Harvesting Endothelial Cells Using Detachable Coils

DANIEL L. COOKE[1], HUA SU[2], ZHENGDA SUN[1], YI GUO[2], DIANA GUO[2], MAYTHEM M. SAEED[1], STEVEN W. HETTS[1], RANDALL T. HIGASHIDA[1], CHRISTOPHER F. DOWD[1], WILLIAM L. YOUNG[2], VAN V. HALBACH[1]

*[1] Department of Radiology and Biomedical Imaging; [2] Department of Anesthesiology and Perioperative Care, University of California; San Francisco, CA, USA*

**Key words:** endothelial, endovascular, aneurysm, brain, stroke, biopsy

## Summary

*The absence of safe and reliable methods to harvest vascular tissue* in situ *limits the discovery of the underlying genetic and pathophysiological mechanisms of many vascular disorders such as aneurysms. We investigated the feasibility and comparable efficacy of endothelial cell collection using a spectrum of endovascular coils.*

*Nine detachable coils ranging in k coefficient (0.15-0.24), diameter (4.0 mm-16.0 mm), and length (8.0 cm-47.0 cm) were tested in pigs. All coils were deployed and retrieved within the iliac artery of pigs (three coils/pig). Collected coils were evaluated under light microscopy. The total and endothelial cells collected by each coil were quantified. The nucleated cells were identified by Wright-Giemsa and DAPI stains. Endothelial and smooth muscle cells were identified by CD31 and α-smooth muscle actin antibody staining.*

*Coils were deployed and retrieved without technical difficulty. Light microscopy demonstrated sheets of cellular material concentrated within the coil winds. All coils collected cellular material while five of nine (55.6%) coils retrieved endothelial cells. Coils collected mean endothelial cell counts of 89.0±101.6. Regression analysis demonstrated a positive correlation between increasing coil diameter and endothelial cell counts ($R^2$=0.52, p = 0.029).*

*Conventional detachable coils can be used to harvest endothelial cells. The number of endothelial cells collected by a coil positively correlated with its diameter. Given the widespread use of coils and their well-described safety profile their potential as an endovascular biopsy device would expand the availability of tissue for cellular and molecular analysis.*

## Introduction

Vascular diseases encompass multiple pathological conditions including, though certainly not limited to, malignancies, arteriovenous malformations and fistulae, inflammatory vasculitides, atherosclerosis, and aneurysms. These various vascular pathologies contain multiple subtypes each with different natural histories and therapeutic algorithms, though all carry significant morbidity and mortality, especially in the brain. However, given the sizable populations affected by vascular disease we still have a limited understanding of the genetic and pathophysiological elements underlying their respective manifestations [1-8].

A major obstacle to solving this problem is the lack of a safe and reliable means to harvest tissue *in vivo*. Biopsy remains an essential diagnostic element for many disease processes, though it is more limited in the central nervous system secondary to procedure-related morbidity. Tissue sampling is helpful in differentiating lesions or areas of suspicious signal on magnetic resonance imaging where malignancy, demyelination, infection, inflammation, and subacute infarction are all possibilities.

To reduced the risk of vessel injury caused

by relative open surgical resection, Feng et al. described a technique for harvesting endothelial cells using a standard endovascular guidewire whereby in the expected usage of the wire and its non-specific contact with the vessel lumen non-circulating endothelial cells bind to the wire [9]. The cells could then be rinsed from the wire and the endothelial population subselected using immunomagnetic beads. The population can then be expanded via culture and studied in any number of ways including examination of messenger RNA. Yu et al. used this technique to harvest coronary artery endothelial cells with similar success, though they noted smaller cell yields per wire ascribed in part to the relatively reduced surface area of the smaller wires [12].

Detachable aneurysm coils share a similar wound outer and flexible inner wire construction to a guidewire, though on a smaller scale. As such, coils contact the endothelium and may bind endothelial cells in a manner similar to that of a guidewire. Coils may in fact exceed many of the cellular collection qualities described for a guidewire. Coils are designed to maximize wire-to-luminal contact by the wall-seeking looping and folding action that occurs as it is placed while a guidewire is designed to minimize contact with the vessel wall and remain within the vascular lumen. Coils have smaller diameters than guidewires and as a result are less traumatic. Finally, given their complex folding geometries, coils may be placed with greater precision than conventional guidewires and in turn provide more specific device-vessel contact. Given these potential benefits we sought to investigate the technical feasibility of endothelial cell harvesting using conventional detachable coils.

## Materials and Methods

### *Animal Preparation*

All animal care procedures were in accordance with the Principles of Laboratory Animal Care formulated by the National Society for Medical Research and the Guide for the Care and Use of Laboratory Animals prepared by the Institute of Laboratory Animal Resources and published by the National Institutes of Health (NIH Publication No. 86-23, revised 1985). All protocols were approved by the IACUC at the University of California San Francisco. Farm pigs weighing 30±2 kg (two to three months old) were purchased and brought into the LARC facility at China Basin at least 48 hours prior to any procedures to acclimate to housing and feeding. Animals were housed individually and fed at a feeding rate of 1.5% to 3% of the animal's body weight daily. Pigs were fasted overnight. Acepromazine (IM) and Ketamine were delivered for premedication. The animals were then transported to the preparation room and placed on isoflurane/oxygen inhalant mask until proper level of anesthesia was obtained at which time the pigs were intubated and maintained using isoflurane/oxygen 2-5%/2-3 L/min. ECG, heart rate, blood pressure, $O_2$-sat, $PCO_2$ and body temperature were monitored during the intervention. Under sterile conditions and fluoroscopic visualization, the iliac artery was approached via the femoral artery.

The animals were returned to the recovery room by experimental staff and monitored until sternal recumbency. The animals required 30-120 minutes for recovery from anesthesia. Experimental staff monitored heart rate, respiratory rate, rectal temp, behavior and indications of pain or discomfort until the animal is sternal. All post-operative drugs were administered and reported by the experimental staff.

### *Coils*

The characteristics of the coils are listed in Table 1. Four of the nine coils used incorporated filaments comprising PGA, a bio-absorbable polymer, within their lumen, a design feature intended to accelerate aneurysmal thrombosis and fibrosis.

### *Cell Harvesting*

Procedures were performed in three animals with three coils assessed per animal. A 19 gauge single wall was used to access the right femoral artery and a 0.035 in Bentson guidewire was used to exchange the needle for a 6F vascular sheath. Under fluoroscopic visualization, a 5F vertebral catheter with an accompanying guidewire was advanced into the right common iliac artery. The wire was withdrawn and the catheter double flushed with normal saline. A Prowler 14 LP microcatheter (Depuy Inc., Raynam, MA, USA) was prepared with a Transcend microwire (Boston Scientific Inc., Natick, MA, USA) and advanced

Table 1 **Coil-based endothelial cell harvesting**

| Coil[1] | Number | Diameter (mm)[2] | Length (cm) | K[3] | Order[4] | Total cell count | Endothelial cell count | ECs/million TCs[5] |
|---|---|---|---|---|---|---|---|---|
| Ultipaq Helical 10 Cerecyte | 1 | 4 | 8 | 0.15 | 1 | 2.5 × 10^6 | 0 | 0 |
| Trufill Orbit complex standard | 2 | 16 | 30 | 0.24 | 2 | 3.2 × 10^7 | 350 | 11 |
| Microsphere Spherical 10 Platinum | 3 | 5 | 9.7 | 0.18 | 3 | 2.4 × 10^5 | 0 | 0 |
| Trufill Orbit complex standard | 4 | 14 | 30 | 0.24 | 1 | 3.7 × 10^6 | 40 | 11 |
| Trufill Orbit complex standard | 5 | 12 | 30 | 0.24 | 2 | 6.3 × 10^5 | 0 | 0 |
| Trufill Orbit complex standard | 6 | 10 | 30 | 0.24 | 3 | 2.2 × 10^7 | 60 | 3 |
| Presidio Spherical 18 Cerecyte | 7 | 16 | 47 | 0.20 | 1 | 4.7 × 10^7 | 285 | 6 |
| Presidio Spherical 18 Cerecyte | 8 | 12 | 40 | 0.20 | 2 | 3.0 × 10^7 | 66 | 2 |
| Presidio Spherical 18 Cerecyte | 9 | 12 | 40 | 0.20 | 3 | 5.8 × 10^5 | 0 | 0 |

*1 All coils were manufactured by Depuy Inc. (Raynam, MA).*
*2 Linear regression of coil diameter relative endothelial cell count R^2 = 0.52, p = 0.029*
*3 K coil "softness" measure spring coefficient ranging from 0 to 1, described by White et al.[13]*
*4 Represents order in which the coil was placed within an animal.*
*5 Number of endothelial cells per million total cells.*
*6 Incorporates filaments comprised of polyglycolic acid (PGA) within the lumen of the microcoils.*

through the guide catheter and positioned within the right common iliac artery. The microwire was removed from the microcatheter. A coil was then advanced, fully unfurled (Figure 1), and then removed from the common iliac artery under fluoroscopic visualization.

After removal from the animal, the coils were cut from their delivery wires and put in tubes containing 25 ml of endothelial cell dissociation buffer (0.5% bovine serum albumin, 2 mmol/L ethylenediaminetetraacetic acid, and 100 µg/ml heparin in calcium- and magnesium-free phosphate buffered saline solution). After incubation for 15 minutes at room temperature, the coils were stretched and rinsed with endothelial dissociation buffer and centrifuged at 2000 RPM for ten minutes at 4°C. The cell pellet was re-suspended in 1 ml PBS. An equal volume of Tryptan blue was added to a 20 ml aliquot of cell suspension. The total viable cells collected by each coil were quantified using a hemocytometer. The cell suspension was then smeared on glass slides (5 ml/slide) and stained with Wright-Giemsa and DAPI for quantification of nucleated cells using a standard protocol.

### *Cell Culture*

A subset of the collected cells were plated in fibronectin (Sigma)-coated culture dishes and cultured in EBM-2 (SingleQuot) with 20% fetal bovine serum for 48 hours at 37°C, 5% $CO_2$.

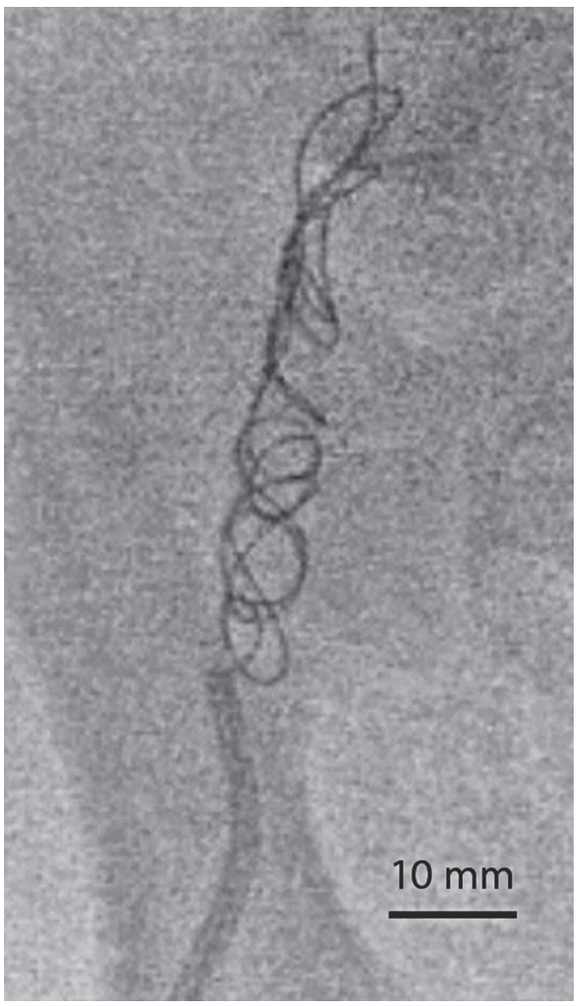


↑ *Figure 1* Coil deployment. Single AP fluoroscopic image of a pig iliac artery demonstrating a 6F guide catheter (arrow) and a 16 mm × 30 cm Trufill Complex standard coil fully deployed within the iliac artery (scale bar: 10 mm).

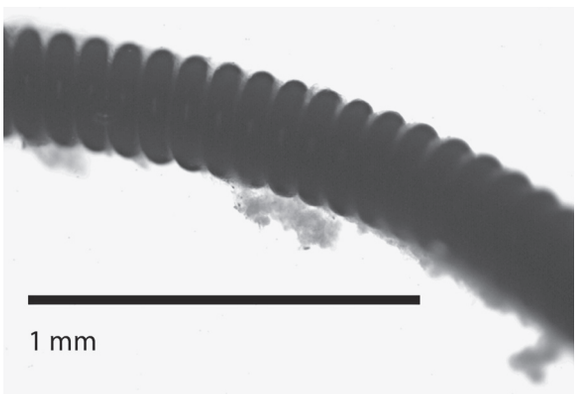


↑ *Figure 2* Cell clusters collected by a coil. Representative light microscopic image demonstrates collections of cellular material along the winds of the coils (scale bar: 1 mm).

### *Immunohistochemistry*

Cultured cells were incubated in medium containing 2.5 µg/ml of 1, 1'-dioctadecyl-3, 3, 3', 3'-tetramethylindocarbocyanine–labeled acetylated low-density lipoprotein (DiI-ac-LDL; Molecular Probes, Eugene, OR) for 1 hour at 37°C, and then fixed with 4% paraformaldehyde for ten minutes. Cells were washed and counterstained with 4', 6-diamidino-2-phenylindole (DAPI) and examined under a fluorescence microscope (Olympus, Japan).

Cell-smears were fixed with 2% PFA for ten minutes, washed with PBS and blocked with 2.5% horse serum for one hour. Cells were incubated with primary antibodies diluted in PBS with 0.1% Triton X-100 overnight at 4°C. The following primary antibodies were used: rabbit anti-human CD31 (BD bioscience, San Diego, CA, USA) von Willebrand Factor (Dako),

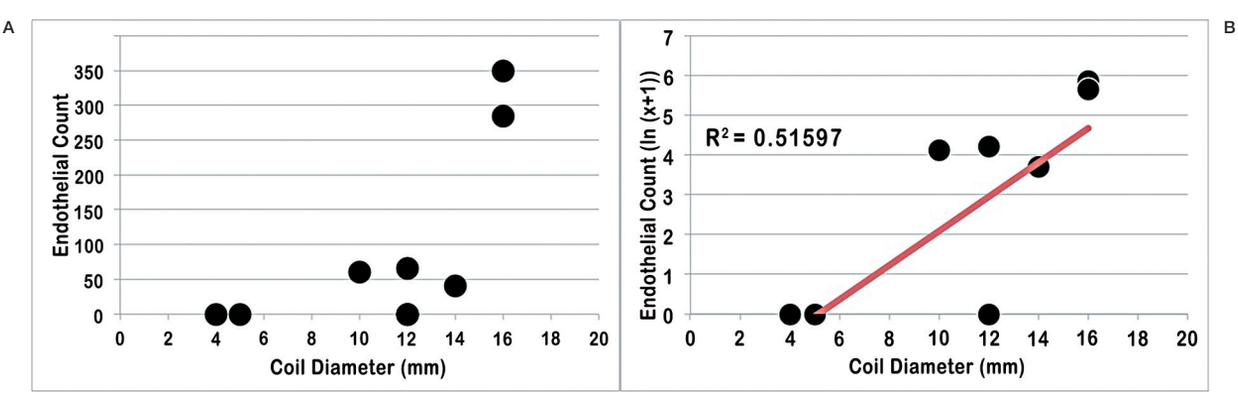


*Figure 3* Endothelial cell count vs. coil diameter. Scatter plot of the raw (A) and log (B) transformation of endothelial cell count (log) (y-axis) relative diameter coil (mm) (x-axis). Note for those cell counts with a zero value the formula ln (x+1) was performed.

CD45 (AbD Serotec) and CD11b (Biolegend) and mouse anti-human alpha-SMA antibody (Sigma), followed by incubation with Alexa Fluor 594-conjugated goat anti-rabbit IgG at 1:500 dilution and Alexa Fluor 488-conjugated goat anti-mouse IgG (Molecular probes, Eugene, OR, USA) at 1:500 dilution for one hour at room temperature. The slides were mounted by Vectorshield Mounting Medium with DAPI (Vector Laboratories) and imaged under a fluorescent microscope. Ten randomly selected fields at 40X were photographed with a fluorescent microscope and endothelial cells and total nuclear cells counted.

*Statistical Analysis*

Coil specifications, deployment order, and total and endothelial cell counts were tabulated in an Excel spreadsheet (Microsoft Inc., Redman, WA, USA). Descriptive statistics were completed within Excel. Statistical analysis of coil characteristics relative to the raw and log(e) transformation of total and endothelial cell counts was performed using Stata software (StataCorp LP, College Station, TX, USA). For those cell counts with a value of zero, logarithmic transformations were performed using the formula, ln(x+1) as there are no zeros on a log scale. Linear regression was performed on k coefficient, diameter, and length. T-test analysis was performed on the presence or absence of PGA coating. Coil characteristic sub-groups were then stratified (Table 2) and statistical analysis performed. ANOVA of k coefficient, diameter, length, and coil-order subgroups relative log transformed total and endothelial cell counts was performed.

## Results

*Coils*

Using conventional detachable-type aneurysm coils, we were able to successfully harvest viable endothelial cells from pig iliac arteries *in*

Table 2 **Coil subgroup analysis**

| Variable[1] | Subgroup (coil number) | Mean (STD) | Total cell count (STD) | p value | Endothelial cell count (STD) | p value |
|---|---|---|---|---|---|---|
| k "softness"[2] | 1 (1,3) | 0.17 (± 0.02) | $1.4 \times 10^6$ (± $1.1 \times 10^6$) | 0.42 | 0.0 (± 0) | 0.30 |
| | 2 (7,8,9) | 0.20 (± 0) | $2.6 \times 10^7$ (± $1.7 \times 10^7$) | | 117.1 (± 112.1) | |
| | 3 (2,4,5,6) | 0.24 (± 0) | $1.5 \times 10^7$ (± $1.2 \times 10^7$) | | 112.5 (± 118.8) | |
| Diameter[3] (mm) | 1 (1,3) | 4.5 mm (± 0.5) | $1.4 \times 10^6$ (± $1.1 \times 10^6$) | 0.26 | 0.0 (± 0) | 0.05 |
| | 2 (5,6,8,9) | 11.5 mm (± 0.75) | $1.3 \times 10^7$ (± $1.3 \times 10^7$) | | 31.5 (± 31.5) | |
| | 3 (2,4,7) | 15.3 mm (± 0.89) | $2.7 \times 10^7$ (± $1.6 \times 10^7$) | | 225.1 (± 123.4) | |
| Length (cm) | 1 (1,3) | 8.9 cm (± 0.85) | $1.4 \times 10^6$ (± $1.1 \times 10^6$) | 0.42 | 0.0 (± 0) | 0.30 |
| | 2 (2,4,5,6) | 30.0 cm (± 0) | $1.5 \times 10^7$ (± $1.2 \times 10^7$) | | 112.5 (± 118.8) | |
| | 3 (7,8,9) | 42.3 cm (± 3.11) | $2.6 \times 10^7$ (± $1.7 \times 10^7$) | | 117.1 (± 112.1) | |
| PGA[4,5] | 1 (1,7,8,9) | | $2.0 \times 10^7$ (± $1.8 \times 10^7$) | 0.63 | 87.8 (± 98.6) | 0.89 |
| | 0 (2,3,4,5,6) | | $1.2 \times 10^7$ (± $1.2 \times 10^7$) | | 90.0 (± 104.0) | |
| Order | 1 (1,4,7) | | $1.8 \times 10^7$ (± $1.9 \times 10^7$) | 0.55 | 108.4 (± 117.9) | 0.63 |
| | 2 (2,5,8) | | $2.1 \times 10^7$ (± $1.4 \times 10^7$) | | 138.7 (± 140.9) | |
| | 3 (3,6,9) | | $7.5 \times 10^7$ (± $9.1 \times 10^6$) | | 20.0 (± 26.7) | |

*[1] Coil characteristic subgroups by k coefficient or "softness", coil diameter in mm, coil length in cm, presence or absence of PGA coating, and order in which the coil was placed into the animal.*
*[2] Coil "softness" measure, spring coefficient ranging from 0 to 1, described by White et al.[13].*
*[3] ANOVA of coil diameter group relative endothelial cell count p = 0.054.*
*[4] 1 denotes coil incorporates filaments comprising polyglycolic acid (PGA) within the lumen of the microcoils.*
*[5] T-test performed in presence (1) or absence (0) of PGA coating relative total and endothelial cell counts.*

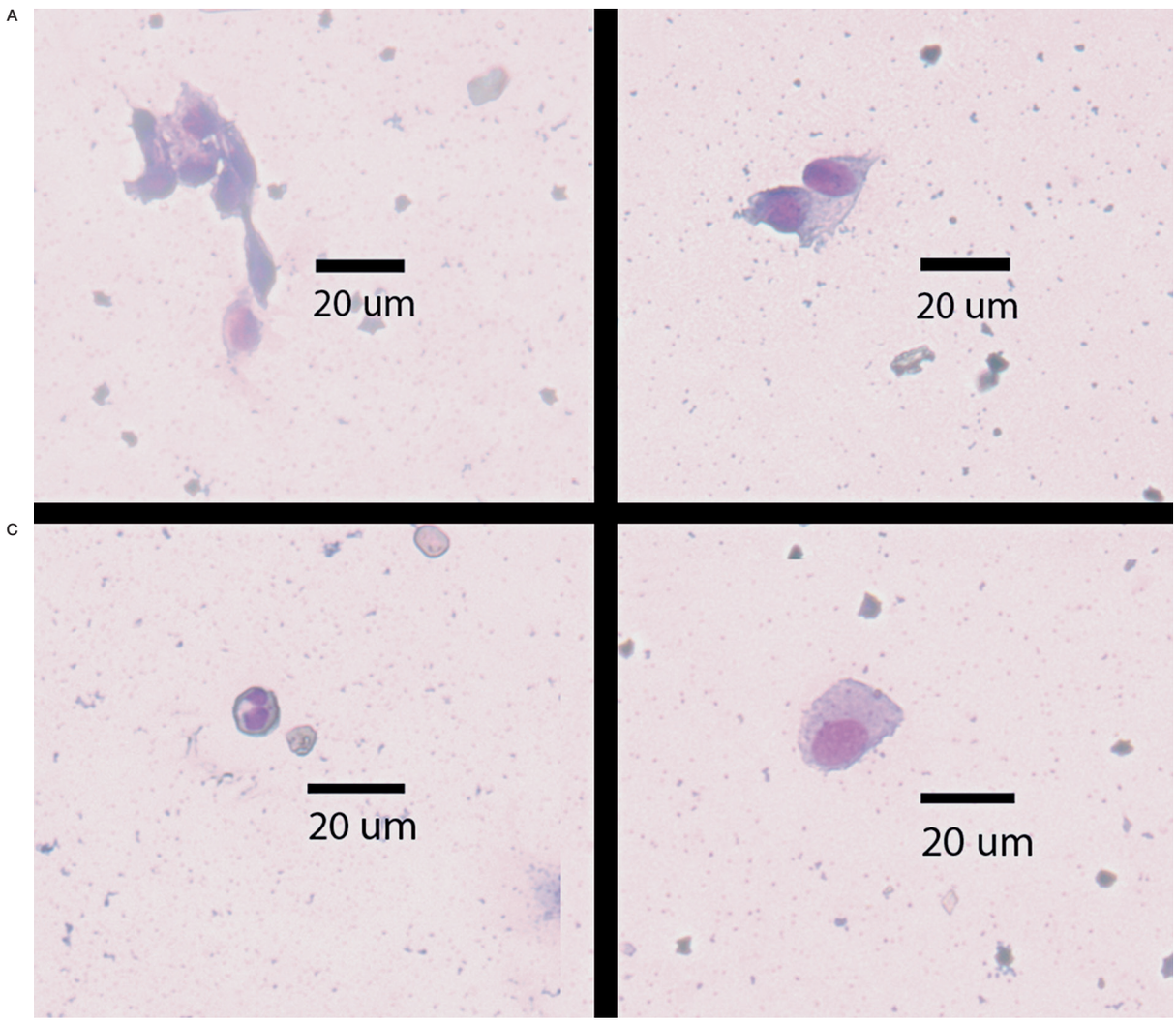


*Figure 4* Nucleated cells collected from coils. Light microscopy Wright-Giemsa staining images demonstrating a collection of nucleated cells (A,B) and individual cells of morphologies consistent with a leukocyte (C) and a monocyte (D) (scale bar: 20 μm).

*vivo*. Nine coils were successfully unfurled within the iliac arteries of live pigs without technical difficulty. The procedures were carried out in three pigs with three different coils placed (Figure 1) and retrieved in successive order per animal (Table 1). Cellular material was detected along the winds of the coils (Figure 2). Though all coils did not harvest endothelial cells (55.6%), all did successfully collect cellular material. The operators noted no difference in coil delivery within order of delivery and all coils assumed the contour of the iliac artery. Longer and wider diameter coils demonstrated subjectively better wall apposition relative to the iliac arteries that tapered from 8.0-6.0 mm in diameter. There was no gross evidence of arterial injury following coil deployment and retrieval.

### *Harvesting Efficiency*

Nine detachable coils ranging in k coefficient (0.15-0.24, mean 0.21 ± 0.03), diameter (4.0 mm-16.0 mm, mean 11.2 ± 3.3), and length (8.0 cm-47.0 cm, mean 29.4 ± 9.1) were used. All coils collected cellular material whereas only five of the nine (55.6%) coils yielded endothelial cells (Table 1). Coils collected mean total and endothelial cell counts of $1.53\times10^7$ ± $1.53\times10^6$ and 89.0 ± 101.6, respectively. Linear regression analysis demonstrated a positive correlation between increasing coil diameter

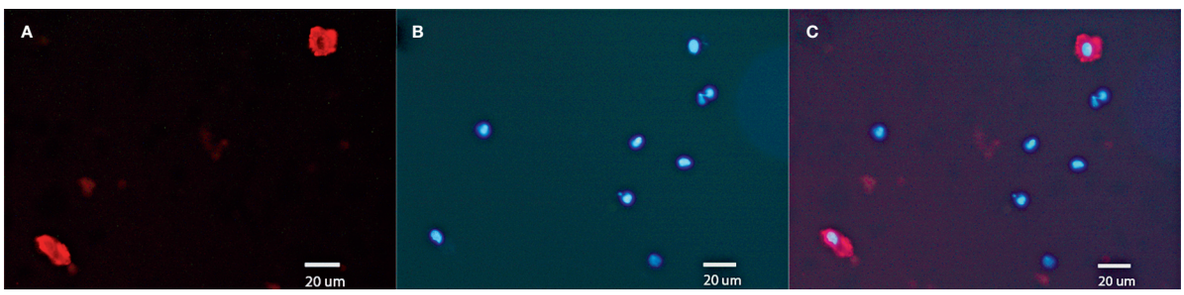


*Figure 5* Nucleated and endothelial cells collected from coils. Microscopic image demonstrating individual CD31 (A) and DAPI (A) and double stained cells (C) (scale bar: 20 μm).

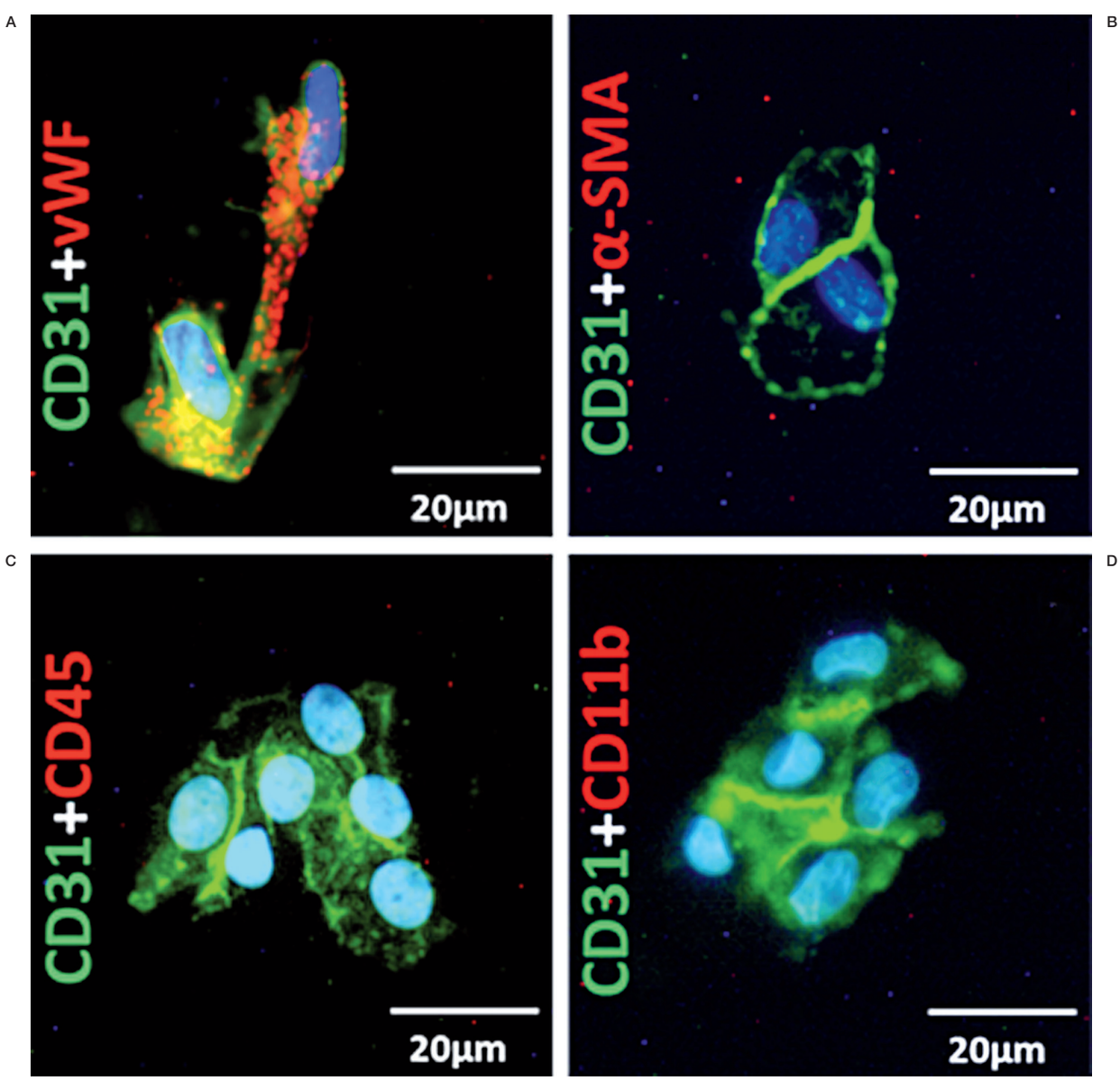


*Figure 6* Double fluorescent staining identify endothelial cells: CD31 co-localizes with vWF (A), but not with α-SMA (B), CD45 (C), or CD11b (D) (scale bar: 20 μm).

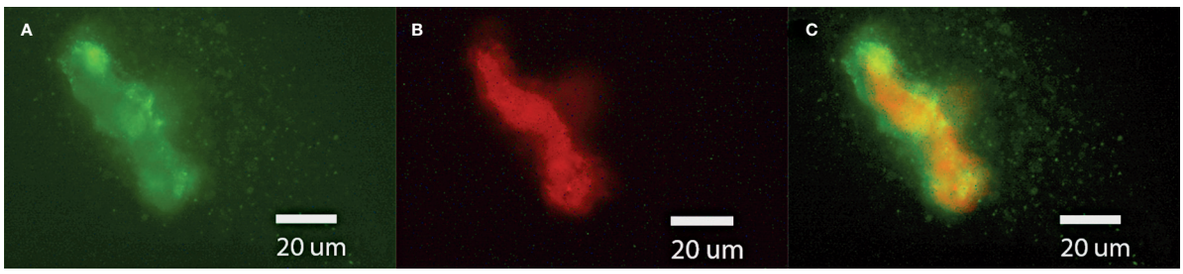


*Figure 7* Immunohistochemistry of alpha smooth muscle and endothelial cells collected from coils. Microscopic images stained for alpha smooth muscle actin (A) and CD31 (B), demonstrating co-localization (C) of these cell types within a cluster of cells taken from a coil (scale bar: 20 μm).

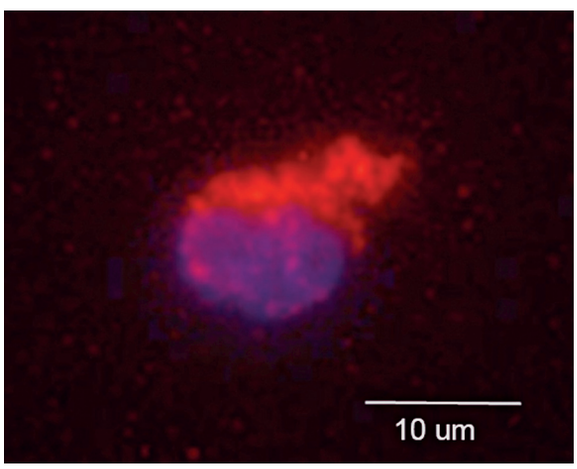


*Figure 8* Surviving endothelial cell with DilAc-LDL uptake (in red). The nuclei were counterstained with DAPI (in blue) (scale bar: 10 μm).

and endothelial cell counts (Figure 3A,B, $R^2$ = 0.52, p = 0.029). Coil length and k coefficient did not demonstrate significant relationships with either total or endothelial cell counts.

Coil subgroup analysis (Table 2) stratified k coefficient, diameter, length, presence or absence of PGA coating, and order of insertion into incremental tiers. Of these subgroups those related to coil diameter (Figure 3) also revealed a trend (p = 0.054) toward an increase in endothelial cell count with increasing coil diameter. Coils from the third tier of the diameter subgroup (Table 2) had a mean diameter of 15.3 mm ± 0.9 and collected 225.1 ± 123.4 endothelial cells per device, the highest endothelial cell counts amongst all subgroups. Coil length, k coefficient, PGA coating, and order of delivery did not demonstrate significant relationships (Table 2) with either total or endothelial cell counts.

### *Characterization of Collected Cells*

The majority of the cells collected were red blood cells. A small fraction of the cells were nucleated of which a subset were endothelial cells. Wright-Giemsa staining demonstrated sheets of nucleated cells (Figure 4A,B) as well as individual leukocytes (Figure 4C) and monocytes (Figure 4D). DAPI staining (Figure 5b) demonstrated nucleated cells with CD31 staining revealing a subset of endothelial cells (Figure 5A,C). Double staining of CD31 positive cells with the alternate endothelial cell marker von Willebrand (vWF) demonstrated co-localization (Figure 6A) while staining (Figure 6C,D) with common leukocyte (CD45) and macrophage (CD11b) markers did not reveal such co-localization. Smooth muscle cells (Figure 7A) and endothelial cells (Figure 7B) were found together within the sheets of cells (Figure 7C). The endothelial cells survived in culture for at least 48 hours (Figure 8).

## Discussion

These experiments serve as a proof of the principle that coils may be a viable alternative endovascular biopsy method. Expectedly, coil diameter proved a significant predicator of endothelial cell yield with larger coils producing

higher endothelial cell tallies. For every mm increase in coil diameter, we estimate a 53% increase in mean endothelial cell count (95% CI: 6-123%). Furthermore, the coil yields from the third tier of the diameter subset are comparable to values published by Feng et al. (262 ± 45 cells per wire) [9]. This may stem from increased force exerted by the coil as it attempts to assume its defined diameter within a confined space. Neither the coil length nor the k coefficient (measure of coil "softness") demonstrated any significant relationship with either total or endothelial cell yield. We found the former result surprising given the considerable differences in surface area between longer and shorter coils. With that in mind, however, it is reassuring that the potential of a coil to harvest endothelial cells be more a measure of the discrepancy between the target vessel and coil diameter than merely the length of the coil itself. This is important given the limitations long coils present as they might only be placed in correspondingly larger vessels or aneurysms. We did not find any effect of the polyglycolic acid-impregnated coils on endothelial collection, though the idea of modifying a coil by varying its pitch, primary and secondary geometries, or surface materials as variables to increase cell yields is intriguing.

It is also noteworthy that circulating endothelial cells may have been collected [13]. Such circulating endothelial cells should be round in shape and though we identified a small number of such cells, the majority of endothelial cells had irregular shapes or formed clusters. These cell clusters also had smooth muscle cells attached (Figure 7), another indicator of their non-circulating origins. Given these observations, we believe the majority of the endothelial cells came directly from the vessel wall. We also note that the harvested cells may be affected by the collection method itself subsequently altering their expected physiology. Prior investigators, using a guidewire endovascular harvesting technique, noted comparable inducible (e.g. lipopolysaccharide-induced E-selectin expression) genetic expression between harvested endothelial cells and cultured control cell populations [9]. Others have also noted comparable expression of housekeeping genes, such as GADPH and vWF, and pro-inflammatory genes between harvested cells and comparable cultured, control cell populations. In future work, we plan to analyze such potential changes by comparing the harvested cells with cultured endothelial cells by immunocytochemical staining and quantitative polymerase chain reaction as well as comparing the isolated cells with the endothelial cells collected from open surgical tissue sections using immunostaining.

Our ultimate goal is to collect endothelial cells from the cerebral vasculature. This study aimed to prove the principal that a coil can collect endothelial cells from an artery in a non-traumatic manner. Future studies might use species large enough to accommodate conventional endovascular devices and without a rete mirabile, the fine mesh-like network found in pigs connecting the extracranial and intracranial arterial systems limiting access to the intracranial vascular anatomy.

Given the significant risk of disability or death related to neurovascular disorders tremendous effort has gone into studying their natural history and treatment. One limitation to further inquiry has been a lack of a safe and reliable means to harvest tissue *in vivo*. Certainly vessels within and surrounding the brain can be collected during open operative intervention, whether an aneurysmal dome or AVM nidus, and undergo genetic analysis. Tissue samples such as these, however, are collected in the setting of treatment providing only a single molecular snapshot of the disease process. Furthermore, the removal of non-pathological intracranial arteries as "normal" control material is prohibited given the stroke risk. As such, dural or extracranial arteries, such as the superficial temporal artery, are used as control samples, though the cellular architecture of such vessels is fundamentally different from the CNS vasculature [15-17]. A method to collect cells from the CNS vasculature, without changing their natural history and over multiple time points would, however, provide vital longitudinal information on mechanisms of disease, in situ biomarkers, and molecular correlates with other clinical and radiographic parameters. A non-traumatic endovascular biopsy method would solve a wide range of questions in vascular biology relevant to clinical management. Its implementation would expand the availability of tissue for genetic analysis to further hone therapeutic targets and metrics to assess clinical risk.

## Conclusion

Neurovascular disease represents a wide spectrum of pathophysiological processes

whose elucidation has been limited to date by lack of a means of safely collecting CNS vascular tissue *in vivo*.

Conventional detachable-type aneurysm coils can successfully collect viable endothelial cells during their routine usage.

The use of such a technique may prove a viable endovascular cell collection method for future study.

**Acknowledgments**

The authors acknowledge Dr. William Dillon and the UCSF Department of Radiology and Biomedical Imaging for their support of the project. The project was supported in part by R01 NS27713, The Aneurysm and AVM Foundation, and Department of Radiology and Biomedical Imaging Seed Grants.

## References

1 Lawton MT, Jacobowitz R, Spetzler RF. Redefined role of angiogenesis in the pathogenesis of dural arteriovenous malformations. J Neurosurg. 1997; 87: 267-274.
2 Chaloupka JC, Marx WF, Kallmes DF. Dural arteriovenous fistulas. J Neurosurg. 2001; 94: 858-861.
3 Krings T, Piske RL, Lasjaunias PL. Intracranial arterial aneurysm vasculopathies: targeting the outer vessel wall. Neuroradiology. 2005; 47: 931-937.
4 Peters DG, Kassam AB, Feingold E, et al. Molecular anatomy of an intracranial aneurysm: coordinated expression of genes involved in wound healing and tissue remodeling. Stroke. 2001; 32: 1036-1042.
5 The Arteriovenous Malformation Study Group. Arteriovenous malformations of the brain in adults. N Engl J Med. 1999; 340: 1812-1818.
6 Moftakhar P, Hauptman J, Malkasian D, et al. Cerebral arteriovenous malformations. Part 1: cellular and molecular biology. Neurosurg Focus. 2009; 26: E10.
7 Vikkula M, Boon L, Mulliken J. Molecular genetics of vascular malformations. Matrix Biol. 2001; 20: 327-335.
8 Mulliken J, Zetter B, Folkman J. In vitro characteristics of endothelium from hemangiomas and vascular malformations. Surgery. 1982; 92: 348-353.
9 Feng L, Stern DM, Pile-Spellman J. Human endothelium: endovascular biopsy and molecular analysis. Radiology. 1999; 212: 655-664.
10 Onat D, Jelic S, Schmidt AM, et al. Vascular endothelial sampling and analysis of gene transcripts: a new quantitative approach to monitor vascular inflammation. J Appl Physiol. 2007; 103: 1873-1878.
11 Feng L, Matsumoto C, Schwartz A, et al. Chronic vascular inflammation in patients with type 2 diabetes: endothelial biopsy and RT-PCR analysis. Diabetes Care. 2005; 28: 379-384.
12 Yu SY, Song YM, Li AM, et al. Isolation and characterization of human coronary artery-derived endothelial cells in vivo from patients undergoing percutaneous coronary interventions. J Vasc Res. 2009; 46: 487-494.
13 Shaffer RG, Greene S, Arshi A, et al. Flow cytometric measurement of circulating endothelial cells: the effect of age and peripheral arterial disease on baseline levels of mature and progenitor populations. Cytometry B Clin Cytom. 2006;70: 56-62.
14 Colombo P, Ashton A, Celaj S, et al. Biopsy coupled to quantitative immunofluorescence: a new method to study the human vascular endothelium. J Appl Physiol. 2002; 92: 1331-1338.
15 Frösen J, Tulamo R, Paetau A, et al. Saccular intracranial aneurysm: pathology and mechanisms. Acta Neuropathol. 2012; 123: 773-786.
16 Aoki T, Nishimura M. The development and the use of experimental animal models to study the underlying mechanisms of CA formation. J Biomed Biotechnol 2011; 2011: 535921.
17 Krings T, Mandell DM, Kiehl TR, et al. Intracranial aneurysms: from vessel wall pathology to therapeutic approach. Nat Rev Neurol. 2011; 7: 547-559.

Daniel L Cooke MD
Dept. of Radiology and Biomedical Imaging
University California San Francisco
505 Parnassus Ave Box-0628
San Francisco, CA 94143, USA
Tel.: +1 415 353-1869
Fax: +1 415 353-8606
E-mail: Daniel.cooke@ucsf.edu